Fluidization of Nanoparticles: A Modified Richardson-Zaki Law

Jose Manuel Valverde and Antonio Castellanos
Dpto. de Electronica y Electromagnetismo. Universidad de Sevilla. Avenida Reina Mercedes s/n, 41012 Sevilla, Spain

DOI 10.1002/aic.10652
Published online September 28, 2005 in Wiley InterScience (www.interscience.wiley.com).

Keywords: fluidization, powders, agglomerates, nanoparticles, fractal structure

Fluidization of nanoparticles is receiving increasing interest as its role is getting bigger in nanopowder-based commercial applications, such as semiconductors, coatings, cosmetics, electronics, sensors, and drug delivery. These particles, which are only about $d_p \sim$ 1-100 nm in size, provide high contact and reaction efficiencies, thus delivering special unique advantages over traditional materials. Even though according to the small size of these particles one would predict Geldart C behavior (impossible to fluidize), there is growing experimental evidence that nanoparticles can be uniformly fluidized for an extended window of gas velocities, that is, primary particle size and density cannot be taken as representative parameters for predicting their fluidization behavior.[1] Empirical investigations reported on fluidization of fine particles agree in that the formation of porous light agglomerates is fundamental to achieve the condition of bubbleless fluidization.[1,2] In our experimental study, we observed that the extension of the nonbubbling fluidization shortened as particle size was increased and shrank to zero in the limit of nonagglomerated particles[2] ($d_p > \sim$ 50 μm).

Yao et al.[3] investigated the fluidization properties of primary 7-16 nm silica nanoparticles. Their SEM study suggested the formation of complex agglomerates by several steps. First, and due to the exceedingly large ratio of interparticle attractive force to particle weight, silica nanoparticles aggregate into branched agglomerates with size $d^* \sim$ 1-100 μm. During fluidization these simple agglomerates join into complex multi-stage agglomerates of equilibrium hydrodynamic size from $d^{**} \approx 230$ μm to $d^{**} \approx$ 330 μm, which can be easily broken up into simple agglomerates by high velocity gas spray. Hakim et. al.[4] used a direct laser imaging system to visualize the dynamics of a fluidized bed of silica nanoparticles and observed highly porous agglomerates continuously breaking up and reforming during fluidization, indicating that the formation of complex agglomerates in the fluidized bed was the result of a dynamic equilibrium process. The existence of multi-stage agglomerates can be the explanation of the apparent discordance reported by Nam et al.[5] between the agglomerate sizes measured by independent methods in their fluidization experiments of $d_p = 12$ nm silica particles. On the one hand, they measured agglomerate sizes of $d^* \approx 30$ μm both by Coulter counter size distribution measurements of the as-received samples and by SEM of agglomerate samples aspirated out of the fluidized bed at different heights. On the other, the agglomerate average hydrodynamic size estimated from pressure drop and bed height data in fluidization experiments was $\approx$160 μm (remarkably similar to the sizes reported by Yao et al.[3]). Likely, the latter belong to the class of multi-stage agglomerates described by Yao et al. while the former are simple agglomerates. As Yao et al. recognize, although the complex agglomerates could be considered as discrete fluidized particles in many circumstances, the fluidization mechanism is much more complicated than that of discrete particles. Our goal in this article is to provide a fundamental perspective on the physics of fluidized beds of nanoparticles. Based on our experience in fluidization of fine micrometric sized particles, which also show aggregation in the fluidized bed,[6] we propose a modified Richardson-Zaki equation for complex agglomerates, along with a straightforward criterion derived from a simple force balance, in order to estimate the equilibrium size of complex agglomerates.

The Richardson-Zaki (R-Z) phenomenological equation[7] is widely accepted to correlate the superficial fluidizing velocity v_g (which for homogeneous fluidization must be equal to the initial settling velocity v_s in sedimentation[7]) and the particle volume fraction ϕ of fluidized beds and suspensions of nonagglomerated particles:

$$\frac{v_s}{v_{p0}} = (1 - \phi)^n \tag{1}$$

v_{p0} being the Stokes settling velocity of a single particle,

$$v_{p0} = \frac{1}{18} \frac{(\rho_p - \rho_f)\, g d_p^2}{\mu} \tag{2}$$

Correspondence concerning this article should be addressed to J.-M. Valverde at jmillan@us.es.

(fluid inertia neglected), where ρ_p is the particle density, ρ_f is the fluid density, g is the gravity field, d_p is the particle size, and μ is the viscosity of the fluid. The exponent n is an empirical parameter whose value has been a subject of discrepancy. For example, Richardson and Zaki reported in their pioneer experimental work $n = 4.65$ in the small particle Reynolds number (Re_t) regime, while n decreased as Re_t increased. Garside and Al Dibouni[8] proposed the empirical relation $(5.1 - n)/(n - 2.7) = 0.1Re_t^{0.9}$. Buscall et al.[9] reported on measurements of the mean fall velocity of sedimenting polystyrene spheres for $Re_t < 1$ over the whole range of values of ϕ and found a best fit to the R-Z law for $n = 5.5$. Rowe[10] fitted experimental data by the law $(4.7 - n)/(n - 2.35) = 0.1Re_t^{3/4}$. A theoretical derivation by Batchelor[11] for $Re_t < 0.1$ using a renormalization method lead him to the equation $v_s/v_{p0} \approx 1\text{-}5.6\phi$, which conforms to the dilute limit by Richardson-Zaki for $n = 5.6$. Snabre and Mills[12] pointed out that n may depend on neglected wall effects, residual polydispersity, and inertial screening, and suggested that due to long range hydrodynamic interactions, there is expected a convergence in the exponent towards $n = 5.6$.

Fine micrometric sized particles agglomerate in the fluidized bed since the ratio of interparticle contact force F_0 to particle weight W_p, $Bo_g = F_0/W_p$ (granular bond number) is still large. The essential difference with fluidization of nanoparticles is that these fluidized agglomerates are simple. Elsewhere we presented an elementary approach to study the fluidized bed of fine powders.[13] We modeled the fluidized bed as an ideal system of simple agglomerates, each one consisting of N primary particles and with a radius of gyration R_G equal to the hydrodynamic radius R_H (let us define $k = 2R_G/d_p$). From this model the settling velocity of the fluidized bed was described by the modified R-Z law:

$$\frac{v_s}{v^*} = (1 - \phi^*)^n \tag{3}$$

where $v^* = v_{p0}N/k$ is the settling velocity of an individual agglomerate and $\phi^* = \phi k^3/N$ is the volume fraction of the agglomerates in the fluidized bed. Thus, this equation may be rewritten as:

$$\frac{v_s}{v_{p0}} = \frac{N}{k}\left(1 - \frac{k^3}{N}\phi\right)^n \tag{4}$$

Since fluidized beds of fine particles are usually operated in the small Reynolds number regime, the best choice in our opinion was to fix $n = 5.6$ in agreement with the theoretical derivation in the dilute limit (we remark, however, that the final results are only weakly dependent on the value of n around $n = 5$). The fit of Eq. 4 to experimental data would give us information of the size and fractal dimension ($D = \ln N/\ln k$) of our fluidized agglomerates. Experiments performed on fine powders[6] with varying particle size (from $d_p \approx 7\mu$m to $d_p \approx 20\ \mu$m) revealed that the size of agglomerates increased with Bo_g according to the power law $N \sim Bo_g^{\alpha}$ ($\alpha \approx 0.7$). The fractal dimension of the agglomerates turned out to be a robust parameter of the fit and always close to $D = 2.5$, as predicted by the diffusion-limited-aggregation (DLA) model (see Figure 1). Moreover, at the fluid-to-solid transition, these low cohesive agglomerates jammed at volume fractions close to the random loose packing of noncohesive spheres[14] ($\phi_J^* \approx \phi_{RLP} \cong 0.56$), as should be expected.

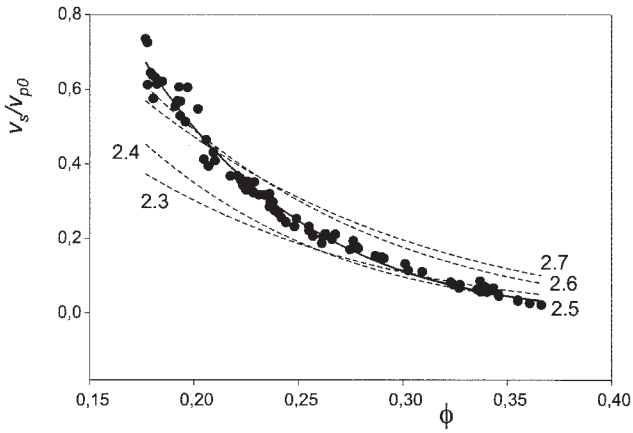

Figure 1. Initial settling velocity v_s (relative to the settling velocity of an individual particle v_{p0}) measured immediately after suddenly stopping the gas flow supply to the fluidized bed vs. the particle volume fraction ϕ of the previously fluidized bed (see[13] for further details on the experimental setup).

The powder consists of 15.4μm polymer particles coated with 32% surface coverage of silica nanoparticles. The continuous line is the best fit of Eq. 4 to the data ($N = 12.4$, $k = 2.72$, $D = \ln N/\ln k = 2.5$). The discontinuous lines are the best fit curves using fixed values of D (indicated) other than D = 2.5.

The equilibrium size of our simple agglomerates in the fluidized bed is determined by the balance between interparticle attractive force and flow shear effects in the gravity field. Gravity is a body force whereas the gas-drag acts mainly at the surface of the agglomerate, thus giving rise to shear forces that are larger the larger the agglomerate. When these shear forces equal the interparticle attractive force, the agglomerate cannot grow anymore. Based on this force balance we derived elsewhere,[15] the criterion

$$Bo_g \sim k^{D+2} \tag{5}$$

For $D = 2.5$, it yields $N \sim Bo^{0.6}$, in close agreement with our experimental results based on sedimentation tests.[6]

We now focus on the problem of fluidization of nanoparticles. In order to obtain the hydrodynamic size of their complex agglomerates, Yao et al.[3] used the original R-Z equation (Eq. 1) and allowed for a variation of the parameter n from $n = 3$ to $n = 7.8$, according to the powder investigated even though the Reynolds number was small in all cases. Then they derived from Eq. 2 the equivalent size of their complex agglomerates, which were considered as effective particles. The same method was adopted by Jung and Gidaspow,[16] who used the agglomerate size obtained in this way as an input to an elaborated simulation aimed to describe the whole collapse process of the bed. Besides the indeterminacy on the parameter n, which we think arises mainly from the fact that they use the volume fraction of the nanoparticles instead of the volume fraction of agglomerates, this approach poses a serious problem: What agglomerate density is employed? Since agglomerates are frac-

tal, their density must decrease with their size. For instance, in the case of simple agglomerates composed of primary particles, we would have $\rho^* = \rho_p N/k^3 = \rho_p k^{D-3}$, and the problem can only get worse for complex agglomerates.

Nam et al.[5] used our modified R-Z equation (Eq. 4); however, in the case of nanoparticles, this equation needs further elaboration since we must take into account that complex agglomerates are formed by aggregation of simple agglomerates in the fluidized bed. Considering these complex agglomerates as effective spheres with density ρ^{**} and size d^{**}, the newly modified R-Z equation to be used should be:

$$\frac{v_s}{v^{**}} = (1 - \phi^{**})^n \tag{6}$$

with

$$v^{**} = \frac{1}{18}\frac{(\rho^{**} - \rho_f)\, g (d^{**})^2}{\mu} \tag{7}$$

v^{**} being the settling velocity of a complex agglomerate and ϕ^{**} the volume fraction of these complex agglomerates in the fluidized bed. Since $\rho^{**} = \rho^* N^*/(k^*)^3 = \rho_p (N/k^3)(N^*/(k^*)^3)$, where N^* is the number of simple agglomerates in the complex agglomerate, $k^* = d^{**}/d^*$, and $\phi^{**} = \phi^*(k^*)^3/N^* = \phi(k^3/N)(k^*)^3/N^*$, Eq. 6 can be rewritten as:

$$\frac{v_s}{v_{p0}} = \frac{N}{k}\frac{N^*}{k^*}\left(1 - \frac{k^3}{N}\frac{(k^*)^3}{N^*}\phi\right)^n \tag{8}$$

This equation is functionally similar to Eq. 4 but conceptually different for it considers explicitly the multiple steps in the formation of complex agglomerates. Thus, the total number of particles agglomerated obtained by Nam et al.,[5] fitting their results to Eq. 4, $N^*N \approx 4 \times 10^{10}$, and the hydrodynamic size of the agglomerates, $d^{**} \approx 160\mu$m, should be interpreted on the basis of Eq. 8. It might well happen that the fractal dimension of the simple agglomerates $D = \ln N/\ln k$ is not the same as the fractal dimension of the complex agglomerates $D^* = \ln N^*/\ln k^*$, which should be close to 2.5, depending on the aggregation mechanism of individual particles in the sample preparation. In that case, the global fractal dimension D^{**} of the complex agglomerate would not be well defined and Eq. 4 would be strictly incorrect from a physical perspective. Nam et al. used Eq. 4, which is equivalent to assuming the same fractal dimension for complex and simple agglomerates, and obtained, however, a reasonable value close to the DLA limit for the global fractal dimension ($D^{**} = \ln(N\,N^*)/\ln(k k^*) \approx 2.57$).

It is worth noting that the complex agglomerates may show even a more intricate hierarchy,[3,17] with nanoparticles linking into a three-dimensional netlike structure, which then coalesce into simple agglomerates of micron size. These simple agglomerates aggregate into complex agglomerates when the bed is fluidized. In this multi-stage agglomerate structure,[3] Eq. 8 should be further extended to take into account the existence of primary agglomerates within the simple agglomerates:

$$\frac{v_s}{v_{p0}} = \frac{N_0}{k_0}\frac{N}{k}\frac{N^*}{k^*}\left(1 - \frac{k_0^3}{N_0}\frac{k^3}{N}\frac{(k^*)^3}{N^*}\phi\right)^n \tag{9}$$

where N_0 is the number of particles aggregated in primary agglomerates, and k_0 is the relative size of these primary agglomerates (related by a fractal dimension $D_0 = \ln N_0/\ln k_0$). Eq. 9 allows us to incorporate in the model any additional knowledge about the multiple aggregation steps that originate the final complex agglomerates. Nevertheless, it must be admitted that, unless there exists available additional information on the different aggregation mechanisms, either Eq. 8 or Eq. 9 might have too many unknown parameters and, therefore, would be impractical.

If we now assume that the limits to aggregation of simple agglomerates into complex agglomerates in the fluidized bed is controlled by the same physical mechanism as for fine micrometric particles, the criterion given by Eq. 5 should be written as

$$Bo_g^* \sim (k^*)^{D^*+2} \tag{10}$$

where $Bo_g^* = F^*/(NW_p)$ is the ratio of the attractive force between simple agglomerates to the weight of a simple agglomerate. These parameters determine the average equilibrium size of the complex agglomerates dynamically formed in the fluidized bed. Once Eqs. 6-10 have been established to analyze the formation of complex agglomerates in fluidized beds nanoparticles, let us test them using reported data in the literature.

The nanopowder used by Nam et al.[5] was Aerosil R974 (Degussa) hydrophobic silica, whose reported particle size d_p, particle density ρ_p, and bulk density ρ_b, are 12 nm, 2200 kg/m^3, and 30 kg/m^3, respectively. According to the global fractal dimension derived D^{**} (close to the DLA limit of 2.5) and the branched highly porous structure observed in the SEM pictures, we might assume for the sake of simplicity that $D^{**} = D^* = D \approx 2.5$. Representative Coulter counter results for pre-experiment powder and SEM pictures of samples aspirated out of the fluidized bed indicated a mean agglomerate size between 30μm and 40μm. Likely, aspiration broke up complex agglomerates into the simple agglomerates that were already present in the as-received sample. Let us write, therefore, $d^* \approx 35\ \mu$m. Thus, $k = d^*/d_p \approx 3 \times 10^3$ and $N = k^D \approx 5 \times 10^8$. The density of the typical simple agglomerate would be $\rho^* = \rho_p N/k^3 \approx 41$ kg/m^3. In a settled bed, these simple agglomerates would pack in a volume fraction ϕ^*_s comparable to the random close packing fraction of hard spheres ($\phi_{RCP} \approx 0.64$) or slightly above because of the soft structure of the nanoparticle agglomerates. Hence, the bulk density of the settled powder would be $\rho_b = \rho^*\phi^*_s \approx 30$ kg/m^3, in accordance with the bulk density value reported. These researchers obtained a hydrodynamic size of agglomerates in the fluidized bed $d^{**} \approx 160\mu$m (analogous to the result from direct measurements using a laser-camera device), which must correspond to the size of the complex agglomerates. Thus $k^* = d^{**}/d^* \approx 4.6$ (note that this value is comparable to the ratio of simple agglomerate size to particle size obtained for our fluidized micrometer sized particles[6]). According to Eq. 10, it should be $Bo_g^* \approx 10^3$ and, hence, the inter-(simple agglomerate) force $F^* \approx 8$nN. Note that the ratio of inter-(complex agglomerate) force to complex agglomerate weight, defined as $Bo_g^{**} \approx Bo_g^*/N^* \sim (k^*)^2$, results in $Bo_g^{**} \sim 10$. Thus, it is justified that complex agglomerates are treated as low cohesive effective spheres in the fluidized bed.

Let us see the accuracy of the force prediction. In order to avoid humidity effects, Nam et al. fluidized their samples with dry nitrogen and the nanoparticles were essentially uncharged; thus, the main source of attraction between particles must be attributed to van der Waals short ranged force[18]:

$$F_{vdW} \approx \frac{A d_p}{24 z_0^2} \tag{11}$$

where A is the Hamaker constant ($A \approx 1.5 \times 10^{-19}$ J for silica[19]], z_0 is the minimum intermolecular distance[18] ($z_0 \approx 4 \times 10^{-10}$m), and d_p is the particle size for nanometric particles. In the case under investigation, $F_{vdW} \approx 0.5$nN. An alternative estimation of the interparticle contact force can be obtained from the interparticle adhesion force:

$$F_{DMT} \approx \pi \gamma d_p \tag{12}$$

where γ is the effective solid surface energy. Eq. 12 was derived by Derjaguin, Muller, and Toporov[20] (DMT) and is appropriate in the limit of small, hard solid particles, such as silica nanoparticles.[21] For these particles, a value of $\gamma \approx 0.04$ J/m^2 has been measured by means of a surface force apparatus.[22] Using this value, we obtain $F_{DMT} \approx 1.5$ nN, which is of the same order of magnitude as the van der Waals force and agrees with the extrapolation of experimental measurements on larger silica particles.[21]

We conclude, therefore, that the interparticle force between silica nanoparticles is $F_0 \approx 1$nN. Since it is expected that simple agglomerates are joined by multiple interparticle contacts, this result proves that the inter-(simple agglomerate) force $F^* \approx 8$nN derived from our model is conceivable. On the other hand, if we think of simple agglomerates as effective micron-sized cohesive particles, the interparticle van der Waals force would be given by $F_{vdW} \approx A d_s/(24 z_0^2)$, where d_s is the typical asperity size of these effective micron-sized particles, entering into the equation due to the short range of action of the van der Waals force. Assuming $F_{vdW} \approx F^*$, one would obtain $d_s \approx 0.2$ μm, which is a reasonable value of the average surface asperity size. (This is the same average asperity size that we use in our calculations of the van der Waals force between polymer micron-sized particles[6].) Nevertheless, it is difficult to give an accurate estimation of the inter-agglomerate force since it should depend on surface structure and configuration of agglomerates, especially if they are highly porous and deformable.

In another work,[23] the same research group (Pfeffer and co-workers) used Eq. 4 to successfully predict the mean agglomerate size for agglomerate particle fluidization (APF) of nanopowders, consisting of smooth, bubbleless, particulate fluidization with high bed expansion. In contrast, the agglomerate sizes predicted for agglomerate bubbling fluidization (ABF), consisting of heterogeneous bubbling fluidization with low bed expansion, were significantly smaller than the agglomerate sizes measured in situ by means of an optical sensor system. They concluded that the model cannot be used to predict the mean agglomerate size of ABF nanoparticles. Let us remark that Pfeffer and co-workers used the superficial gas velocity v_g instead of the settling velocity v_s as an input parameter in Eq. 4. Certainly the measurement of v_g, which is controlled by the imposed gas flow, is much easier than the measurement of v_s since for the latter purpose settling experiments, implying continuous measurement of the bed height when the gas supply is shut off, must be carried out. While both velocities are similar in the regime of homogeneous fluidization, v_g is clearly larger than v_s in the bubbling heterogeneous regime[13] because bubbles and/or channels allow for a bypass of an appreciable volume of gas, thus curtailing further expansion of the bed.

We carried out measurements of v_s on highly cohesive micropowders displaying heterogeneous fluidization, but the big scatter of the data prevented us from a confident measurement of the agglomerate size.[15] According to the rather large compression index values measured for these powders in compaction tests at very low pressures,[15] we arrived at the conclusion that porous agglomerated fragments that earlier existed as aggregates in the previously loaded powder should persist in fluidization, thus giving rise to exceedingly large clusters of strongly adhered particles in the heterogeneously fluidized state. This was confirmed by an estimation of k from the data on the fluid-to-solid (jamming) transition: $k^D/k^3 \approx \phi_J/\phi^*_J$. In this equation the most important and variable parameter is ϕ_J, which is the particle volume fraction at the transition to solid and could be measured. ϕ^*_J is the volume fraction filled by the agglomerates, which due to the small inter-agglomerate cohesion was slightly below 0.56 (random loose packing of noncohesive hard spheres). The values of k estimated in this way were consistent with the predicted law of compaction at low consolidations.[15] Yet they were considerably larger than those predicted by Eq. 5 if the interparticle force in fluidization was simply assumed to be the van der Waals force. This result strongly suggests that, due to contact plasticity, interparticle contacts within the big agglomerates retained memory of the loaded state before fluidization, i e., fluidization was not able to break all interparticle contacts of the previously loaded solid. Therefore, it must be considered that for very cohesive powders, the interparticle attractive force in the fluidized bed may be locally much higher than the interparticle van der Waals force.

This memory effect (due to plasticity in our case, in other cases humidity, aging, etc.) can be erased as, for example, Nam et al. did,[5] who coupled aeration with vibration, thus achieving homogeneous smooth expansion due to the breakup of history-dependent, excessively large and cohesive, not simple agglomerates. The reader may check that, for the same nanopowder (Aerosil R974), the mean agglomerate size measured without using initial vibration[23] (315 μm) was about twice the value measured by previously vibrating the bed[5] (160 μm). Quite remarkably, this research group has shown that smooth fluidization of Aerosil R974 can also be enhanced with the assistance of magnetic particles in an oscillating magnetic field[24] or sound wave excitation at low frequencies,[25] while the mean agglomerate size is decreased to comparable values to the vibration assisted fluidization. With the aid of magnetic excitation, the fluidization pattern of nanopowders with larger than 500 μm agglomerates can be changed from ABF to APF fluidization, which implies agglomerate size reduction.[24] Thus, vibration, magnetic, or sound assisted fluidization erase the powder memory, allowing for a dynamic aggregation mechanism of simple agglomerates into complex agglomerates controlled by a DLA process and size-limited by Eq. 10.

Matsuda et al.[26] have recently reported on the effect of varying the effective gravitational acceleration g_{ef} by means of a centrifugal fluidized bed on the size of fluidized agglomerates. From data on the minimum fluidization velocity and

empirical correlations with the Reynolds and Arquimedes numbers, they inferred the agglomerate size, which was related to g_{ef} by means of the equation $d^{**} \propto g_{ef}^{-0.4}$. Even though they proposed an interesting energy balance equation to predict this law, their result is based on assuming that there exists an attainable energy for disintegration of agglomerates E_a proportional to g_{ef}^{n}, where n is adjusted to 0.4 to fit the model to their experimental results. Moreover, in their derivation of agglomerate size, they assumed that the agglomerate density ρ^{**} can be approximated by the tapped density of the bed ρ_T in calculating the Arquimedes number of the agglomerate Ar:

$$Ar \approx \frac{(d^{**})^2 \rho_f (\rho_T - \rho_f) g_{ef}}{\mu^2} \tag{13}$$

Since probably they had complex agglomerates, it is more accurate to write $\rho^{**} = \rho^* N^*/(k^*)^3 = \rho^*(k^*)^{D-3}$ (note that it depends on the size of the complex agglomerate, $k^* = d^{**}/d^*$), while the tapped density of the bed is obtained by a close random packing of the simple agglomerates, thus $\rho_T = \rho^* \phi_{RCP,}$ where $\phi_{RCP} > \sim 0.64$. Therefore, $\rho_T = \rho^{**}(k^*)^{3-D}\phi_{RCP}$. If we neglect fluid density (valid for gas-fluidization), we may write in Eq. 13 $(\rho_T - \rho_f) g_{ef} \approx \rho_T g_{ef} = \rho^{**}(g_{ef}\rho_T/\rho^{**}) = \rho^{**}[(k^*)^{3-D}\phi_{RCP} g_{ef}]$. If ρ^{**} would have been considered instead of ρ_T in Eq. 13, Matsuda et al.'s result should be rewritten as $d^{**} \propto [(d^{**})^{3-D} g_{ef}]^{-0.4}$. Hence, $d^{**} \propto g_{ef}^{-0.33}$ using $D = 2.5$.

Let us see the prediction of our model. From Eq. 10, we obtain $d^{**} \propto g_{ef}^{-1/(D+2)} \approx g_{ef}^{-0.22}$, which is close to the experimental result without any assumption needed other than the fractal dimension of the agglomerates being close to the DLA limit ($D = 2.5$), as most experiments indicate. It must be also noted that, since Matsuda et al. did not use external assistance to erase the powder memory, history dependent agglomerates could be progressively broken as g_{ef} was increased, which would be reflected in Eq. 10 in an effective decrease of the average interparticle force, thus leading to a more rapid decrease of the average agglomerate size with g_{ef}.

In conclusion, motivated by the growing evidence on the formation of complex agglomerates in homogeneously fluidized beds of nanoparticles, and based on a simple physical model, we propose Eqs. 8 and 10 for the estimation of relevant parameters, such as complex agglomerate size, fractal dimension, and inter-(simple agglomerate) force. According to the experimental studies recently published, it seems obvious that simple agglomerates are present in the as-received sample before being subjected to fluidization and can be, therefore, characterized by SEM or other sizing method analysis. Complex agglomerates are formed by a dynamic equilibrium process in the fluidized bed governed by a balance between inter-(simple agglomerate) attractive force and flow shear.

Acknowledgments

This research has been supported by Xerox Foundation and Spanish Government Agency Ministerio de Ciencia y Tecnologia (contract BFM2003–01739).

Literature Cited

1. Yang WC. Fluidization of fine cohesive powders and nanoparticles—a review. *J Inst Chem Engrs.* 2005;36:1-15.
2. Valverde JM, Castellanos A, Mills P, Quintanilla MAS. Effect of particle size and interparticle force on the fluidization behavior of gas-fluidized beds. *Phys Rev E.* 2003;67:051305 (1–6).
3. Yao W, Guangsheng G, Fei W, Jun W. Fluidization and agglomerate structure of SiO_2 nanoparticles. *Powder Technol.* 2002;124:152–159.
4. Hakim LF, Portman JL, Wank JR, Buechler KJ, Weimer A. High Speed Laser Imaging Processing for Investigating Fluidized Nanoparticles. AIChE Annual Meeting, San Francisco, CA, November 16-21, 2003.
5. Nam CH, Pfeffer R, Dave RN, Sundaresan S. Aerated vibrofluidization of silica nanoparticles. *AIChE J.* 2004;50:1776-1785.
6. Castellanos A, Valverde JM, Quintanilla MAS. Aggregation and sedimentation in gas-fluidized beds of cohesive powders. *Phys. Rev. E.* 2001;64:041304 (1–7).
7. Richardson JF, Zaki WN. Sedimentation and fluidization: Part I. *Trans Inst Chem Engrs.* 1954;32:35-53.
8. Garside J, Al-Dibouni MR. Velocity-voidage relationships for fluidization and sedimentation in solid-liquid systems. *Ind Eng Chem Process Des Develop.* 1977;2:206-214.
9. Buscall R, Goodwin JW, Ottewill RH, Tadros TF. The settling of particles through newtonian and non-newtonian media. *J Colloid Interface Sci.* 1982;85:78-86.
10. Rowe PN. A convenient empirical-equation for estimation of the Richardson-Zaki exponent. *Chem Eng Sci.* 1987;42:2795-2796.
11. (a) Batchelor GK. Sedimentation in a dilute polydisperse system of interacting spheres. 1. General theory. *J Fluid Mech.* 1982;119:379-408. (b) Batchelor GK, Wen CS. Sedimentation in a dilute polydisperse system of interacting spheres. 2. Numerical results. *J Fluid Mech.* 1982;124:495-528.
12. Snabre P, Mills P. Settling and fluidization of non Brownian hard spheres in a viscous liquid. *Eur Phys J E.* 2000;1:105-114.
13. Valverde JM, Quintanilla MAS, Castellanos A, Mills P. The settling of fine cohesive powders. *Europhys Lett.* 2001;54:329-334.
14. Valverde JM, Castellanos A, Quintanilla MAS. Jamming threshold of dry fine powders. *Phys Rev Lett.* 2004;92:258303 (1–4).
15. Castellanos A, Valverde JM, Quintanilla MAS. Physics of compaction of fine cohesive powders. *Phys Rev Lett.* 2005;94:75501 (1–4).
16. Jung J, Gidaspow D. Fluidization of nano-size particles. *J Nanopart Res.* 2002;4:483-497.
17. R. Pfeffer, private communication.
18. Krupp H. Particle adhesion. Theory and experiment. *Adv Colloid Interface Sci.* 1967;1:111-239.
19. Ross S, Morrison ID. *Colloidal Systems and Interfaces*. New York: Wiley-Interscience; 1988.
20. Derjaguin BV, Muller VM, Toporov YP. Effect of contact deformations on adhesion of particles. *J Colloid Interface Sci.* 1975;53:314-326.
21. Heim LO, Blum J, Preuss M, Butt HJ. Adhesion and friction forces between spherical micrometer-sized particles. *Phys Rev Lett.* 1999;83:3328-3331.
22. Horn RG, Smith DT, Haller W. Surface forces and viscosity of water measured between silica sheets. *Chem Phys Lett.* 1989;162:404-408.
23. Zhu C, Yu Q, Dave RN, Pfeffer R. Gas fluidization characteristics of nanoparticle agglomerates. *AIChE J.* 2005;51:426-439.
24. Yu Q, Dave RN, Zhu C, Quevedo JA, Pfeffer R. Enhanced fluidization of nanoparticles in an oscillating magnetic field. *AIChE J.* 2005;51:1971-1979.
25. Zhu C, Liu G, Yu Q, Pfeffer R, Dave RN, Nam CH. Sound assisted fluidization of nanoparticle agglomerates. *Powder Technol.* 2004;141:119-123.
26. Matsuda S, Hatano H, Muramoto T, Tsutsumi A. Modelling for size reduction of agglomerates in nanoparticle fluidization. *AIChE J.* 2004;50:2763-2771.

Manuscript received May 27, 2005, and revision received July 4, 2005.